http://dx.doi.org/10.5516/NET.01.2014.709

PROPAGATION OF NUCLEAR DATA UNCERTAINTIES FOR PWR CORE ANALYSIS

O. CABELLOS*, E. CASTRO, C. AHNERT, and C. HOLGADO
Department of Nuclear Engineering, Universidad Politécnica de Madrid
C/José Gutiérrez Abascal, 2, 28006, Madrid, Spain
*Corresponding author. E-mail : oscar.cabellos@upm.es

Received September 26, 2013

An uncertainty propagation methodology based on the Monte Carlo method is applied to PWR nuclear design analysis to assess the impact of nuclear data uncertainties. The importance of the nuclear data uncertainties for ^{235,238}U, ^{239}Pu, and the thermal scattering library for hydrogen in water is analyzed. This uncertainty analysis is compared with the design and acceptance criteria to assure the adequacy of bounding estimates in safety margins.

KEYWORDS : Uncertainty Propagation, Nuclear Data, Fuel Cycle, Design and Acceptance Criteria, PWR

1. INTRODUCTION

The SEANAP system developed and applied for 3-D PWR core analysis has demonstrated a very good agreement with the broad sets of parameters and cycles analyzed at the Spanish PWR units [1, 2, 3]. Thus, a rather small calculational uncertainty appears when comparing calculations with reactor operation data measurements, such as core start-up tests. SEANAP validation of the critical boron concentrations along many completed operating cycles show that the calculated values are within 20-50 ppm of the measured values, the calculated axial asymmetry of incore power is within 1-4% including the cycle start-up and operation maneuvers at different powers along the whole cycle. In addition, the differences between calculated and measured assembly relative powers at several burnups are within 2-5%.

However, this global calculational uncertainty relies on many different sources of uncertainty: models and methods, but also in nuclear data. Consequently, the importance of nuclear data uncertainties to operation and safety core design parameters has to be assessed in order to yield realistic uncertainty values.

To perform a full propagation from nuclear data uncertainties, some methodologies based on the Monte-Carlo approach [4,5 and 6] have been proposed together with the former deterministic techniques based on perturbation methods [7,8]. The Total Monte Carlo (TMC) method, developed by NRG [6] for nuclear data uncertainty propagation, consists of a repeated reactor calculation, randomly varying the entire nuclear data library each time. The random set of nuclear data files used in this work is ^{235,238}U, ^{239}Pu [9] based on TENDL2012 [10] and Thermal Scattering Library for Hydrogen in Water (STL-H in H2O) [11].

2. DESCRIPTION OF THE CORE MODEL

The uncertainty analysis has been applied to the core design in a 3-loop Westinghouse 900 MWe PWR unit. The cycle assessed in this work has a loading pattern of 157 fuel assemblies (FA), with two different types: AEF- Advanced European Fuel and OFA- Westinghouse Optimized Fuel Assembly. All FA types have the same configuration, 17x17 with 24 guide thimbles and 1 instrumentation thimble at the center. A set of 40 different FAs are considered for the neutron transport lattice calculation according to type of FA (AEF, OFA), enrichment (2.1, 3.1, 3.24 and 3.6 w/o), level of burnup, and burnable absorbers (4, 8, or 12 WABAs -wet annular burnable absorbers per FA). Fig. 1 shows a set of 22 different types of FA without control rods in the loading pattern of ¼ core. The location of control rods in the core is used to define an additional set of 9 types of FA with Ag-In-Cd and 9 FAs with B4C, because of the hybrid design of B4C absorbers with an Ag-In-Cd absorber in the lower portion of the control rod. More detailed information for all the sets of FAs is given in Table 1.

The SEANAP system used for this study is integrated by three interconnected subsystems or codes: the MARIA [1] subsystem for FA calculations, the COBAYA code [2] for detailed (pin-by-pin) two-dimensional core calculations at reference conditions, and the SIMULA subsystem [1] for three-dimensional one-group corrected-nodal core simulation. A scheme of the system is shown in Fig. 2.

The MARIA subsystem integrates the PREWIM, WIMS-D4 [12], and POSWIM codes. The PREWIM code generates the complete input data files required by the WIMS-D4 code, in a consistent and efficient way, for all sets of FA calculations covering the parameter space of the local physical variables (water density, fuel temperature,

1	13	4	21	6	21	16	14
13	11	15	2	16	6	20	7
4	15	3	21	8	22	19	
21	2	21	9	18	20	5	
6	16	8	18	12	17		
21	6	22	20	17			
16	20	19	10				
14	7						

		C				D	
	SB				SA		
C		D		B		A	
			SB				
		B		C			
	SA						
D		A					

Fig. 1. Assembly Distribution in the Loading Pattern ¼ Core (Left). Location of Control Rod Banks (Right).

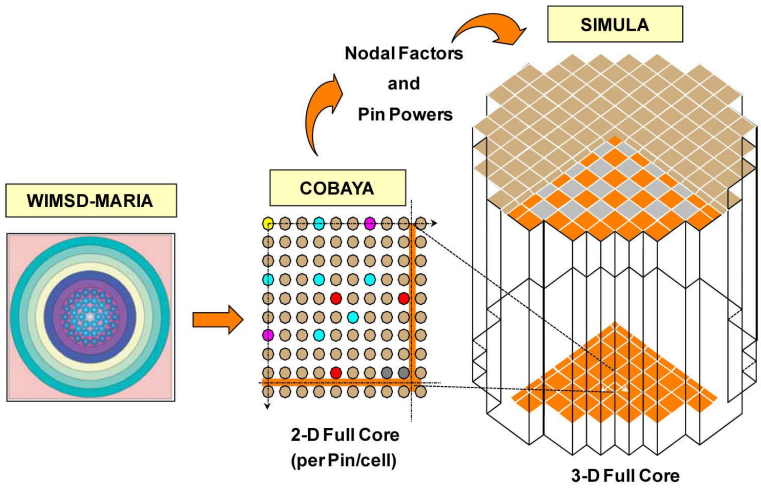

Fig. 2. Scheme of the PWR Core Analysis System SEANAP: WIMS-D4, COBAYA, and SIMULA Coupling.

xenon concentration, boron concentration, burnup, and control) along each cycle of reload and operation. Fuel assemblies are modeled using a cylindrical model of the equivalent fraction of each FA type. This modelization provides an efficient and accurate treatment of the PWR fuel assembly with regularly distributed fuel rods, water tubes, and control rods or burnable absorber tubes. The WIMS-D4 lattice code calculates the PWR fuel assembly in the annular cluster geometry by SN neutron transport calculation. The WIMS-D4 code uses an original nuclear data library in 69 energy groups, but for this modelization a weighted energy library of 24 energy groups is used. The transport fluxes in 24 energy groups are used for weighting the two-group cross sections by whole assemblies and by pin-cell type. The libraries per cell type include: macroscopic cross sections, microscopic cross-sections of the relevant nuclides boron, xenon, samarium, and water, delayed neutron fractions, and fission product yields.

COBAYA is a pin-by-pin 2D code (calculations of full core planes, including radial reflector) with a finite difference two-group diffusion method. Some selected calculations for core conditions and configurations along the cycle, including several unrodded and rodded configurations at Hot Zero Power (HZP) and Hot Full Power (HFP), at several burnup steps from Begin of Cycle (BOC) to End of Cycle (EOC), are performed. COBAYA processes the successive cases with changes in the core configuration obtaining the explicitly calculated spectral and transport correction nodal discontinuity factors, average and relative albedoes at the core boundary, and hot-pin to node average power ratios to be input directly into the core simulator SIMULA.

SIMULA is a nodal 3D code (four nodes per fuel assembly and axial mesh of 34 nodes), with a simplified close-channel subcooled-water thermalhydraulics. This code implements a linear-discontinuous finite-difference scheme for synthetic coarse-mesh few group diffusion calculation. The synthetic nodal discontinuity factors in

Table 1. Reactivity Uncertainty of FAs at BOC, HFP, and C_B=1348 ppm

#	Fuel Assembly	# Burnup Absorbers/ Control Rods	Enrichment (w/o)	Burnup at BOC (GWD/TMU)	Average Kinf	Δk/k% due to:				
						STL	^{239}Pu	^{235}U	^{238}U	TOTAL
1	OFA	-	2.1	18147	0.91360	0.18	0.50	0.37	0.28	0.70
2	OFA	-	3.1	28827	0.89790	0.27	0.52	0.29	0.27	0.70
3	OFA	-	3.24	27054	0.93579	0.26	0.46	0.31	0.27	0.67
4	OFA	-	3.24	27519	0.96487	0.24	0.42	0.34	0.26	0.65
5	OFA	-	3.24	29887	0.96398	0.25	0.44	0.34	0.26	0.66
6	OFA	-	3.24	29340	0.96465	0.25	0.43	0.33	0.26	0.66
7	OFA	-	3.24	30232	0.96227	0.26	0.45	0.32	0.26	0.66
8	OFA	-	3.24	22908	0.98784	0.25	0.40	0.35	0.26	0.65
9	OFA	-	3.24	30456	0.94295	0.27	0.47	0.30	0.26	0.67
10	OFA	-	3.24	30053	0.96551	0.26	0.44	0.32	0.26	0.66
11	OFA	-	3.24	16273	1.09368	0.15	0.23	0.49	0.26	0.62
12	AEF	-	3.6	13050	1.13885	0.14	0.16	0.50	0.28	0.61
13	AEF	-	3.6	11577	1.14386	0.14	0.15	0.51	0.28	0.61
14	AEF	-	3.6	11695	1.12998	0.16	0.18	0.48	0.28	0.61
15	AEF	-	3.6	13263	1.13845	0.15	0.17	0.49	0.28	0.61
16	AEF	-	3.6	13285	1.13486	0.15	0.18	0.48	0.28	0.60
17	AEF	-	3.6	15024	1.11838	0.18	0.22	0.45	0.28	0.60
18	AEF	-	3.6	15233	1.12937	0.16	0.19	0.47	0.28	0.60
19	AEF	-	3.6	0	1.21566	0.09	0.00	0.63	0.27	0.69
20	AEF	4 WABAS	3.6	0	1.18455	0.12	0.00	0.64	0.27	0.71
21	AEF	8 WABAS	3.6	0	1.15216	0.15	0.00	0.65	0.27	0.72
22	AEF	12 WABAS	3.6	0	1.12014	0.18	0.00	0.66	0.27	0.73
23	OFA	CTL-Ag-In-Cd	3.24	27054	0.68538	0.63	0.48	0.30	0.27	0.90
24	OFA	CTL-Ag-In-Cd	3.24	27519	0.70843	0.62	0.45	0.33	0.27	0.88
25	OFA	CTL-Ag-In-Cd	3.24	29340	0.71012	0.62	0.45	0.32	0.27	0.88
26	OFA	CTL-Ag-In-Cd	3.24	22908	0.72835	0.62	0.43	0.34	0.27	0.87
27	OFA	CTL-Ag-In-Cd	3.24	30456	0.69436	0.64	0.49	0.29	0.27	0.89
28	OFA	CTL-Ag-In-Cd	3.24	16273	0.80665	0.56	0.25	0.48	0.26	0.82
29	AEF	CTL-Ag-In-Cd	3.6	13050	0.85273	0.53	0.18	0.49	0.28	0.80
30	AEF	CTL-Ag-In-Cd	3.6	13285	0.85183	0.54	0.19	0.47	0.28	0.79
31	AEF	CTL-Ag-In-Cd	3.6	0	0.90497	0.53	0.00	0.65	0.26	0.88
32	OFA	CTL-B4C	3.24	27054	0.62228	0.69	0.47	0.29	0.27	0.93
33	OFA	CTL-B4C	3.24	27519	0.64298	0.67	0.44	0.32	0.27	0.91
34	OFA	CTL-B4C	3.24	29340	0.64454	0.68	0.44	0.31	0.27	0.91
35	OFA	CTL-B4C	3.24	22908	0.66091	0.67	0.42	0.33	0.27	0.90
36	OFA	CTL-B4C	3.24	30456	0.63041	0.69	0.48	0.28	0.27	0.92
37	OFA	CTL-B4C	3.24	16273	0.73125	0.61	0.25	0.47	0.26	0.85
38	AEF	CTL-B4C	3.6	13050	0.77150	0.59	0.17	0.47	0.28	0.82
39	AEF	CTL-B4C	3.6	13285	0.77077	0.59	0.19	0.46	0.28	0.82
40	AEF	CTL-B4C	3.6	0	0.82126	0.59	0.00	0.63	0.26	0.90

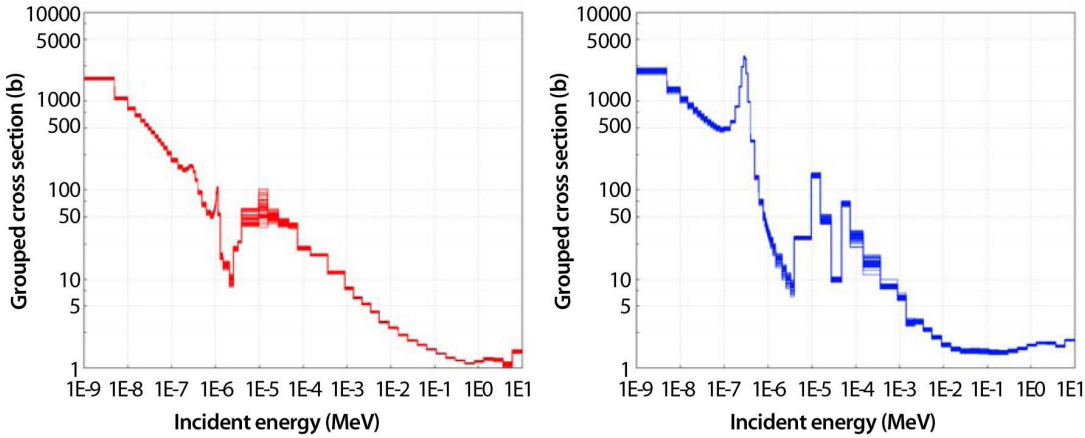

Fig. 3. First 50 Random Multigroup Fission Cross-sections for ^{235}U (Left) and ^{239}Pu (Right) Processed with NJOY/GROUPR at 293K with Infinite Dilution.

the X-Y directions are provided by the COBAYA code, for each node type as a function of node burnup, from 2D average core plane calculations of the cycle nominal burnup and rodded combinations.

The SEANAP system has been applied in the last 25 years in 7 Spanish PWR units (Almaraz I and II, Ascó I and II, Trillo, Vandellós II and Zorita). The scope of applications integrated in SEANAP covers: i) fuel loading pattern optimization carried out for about 75 cycles with very positive results, ii) full capability of the nuclear design for each cycle: start-up physics test at HZP (critical end-point boron concentration, isothermal temperature coefficients, control bank worths, differential boron worth, and power distribution) and nominal operation (boron concentration, 1D and 2D power distributions from in-core flux maps), iii) the SEANAP system has been developed and implemented as an online simulator used in ~20 cycles of three PWRs (Vandellós-II, Ascó-I, and Ascó-II). The main capabilities of this online simulator are summarized as follows: continuous operational surveillance every 5 minutes (boron concentration, reaction rates at the excore detectors, Axial Offset (AO), fluid temperatures at the location of thermocouples, temperatures at the hot legs…), incore/excore calibrations, monthly incore flux maps, and planning of optimal maneuvers with dynamic core analysis for safety and training for plant engineers and operators.

3. UNCERTAINTY PROPAGATION

3.1 Nuclear Data Uncertainties

Nuclear data uncertainties are taken from the TENDL 2012 random nuclear data files using these files to repeat identical simulations with different nuclear data. Random nuclear data files are provided in the ENDF-6 format for reactions induced by neutrons up to 20 MeV. In this work random files for STL-H in H2O (~800 randoms), ^{235}U (~740 randoms), ^{238}U (~700 randoms) and ^{239}Pu (~740 randoms) are used. In the ^{235,238}U and ^{239}Pu random files, all the nuclear data (cross sections, angular distributions, double differential data, gamma and neutron emissions, isomeric ratios, and for actinides nu-bar and fission neutron spectra) are randomly varied from fundamental theoretical nuclear quantities with the help of a nuclear reaction code, TALYS [9].

For STL-H in H2O only the incoherent inelastic scattering component of the thermal neutron scattering is considered, and the coherent and incoherent elastic scattering can be neglected. Then, seven parameters of the thermal scattering data S(α, β) are randomized. The central values of these parameters are the ones used for JEFF-3.1.1, assuming a uniform probability distribution using uncertainty values which reproduce the experimental uncertainty of the thermal scattering cross-section for H in H2O [11]. This is the whole idea behind TMC [6].

These random files are processed with NJOY [13]. The GROUPR and WIMSR modules of NJOY are used. The WIMSR module of NJOY is needed to process the random files to be used by the WIMS-D4 code. After generation of random files processed with NJOY/WIMSR for ^{1}H, ^{235,238}U, and ^{239}Pu, the WILLIE program [14] is used for including each data file into the reference WIMS-D4 library. It provides a set of random WIMS-D4 libraries updated with new random data for each of these materials: ^{1}H, ^{235,238}U, and ^{239}Pu.

The GROUPR module is used to process these files into a multigroup energy structure for the WIMSR module. Furthermore, multigroup cross-section data are used for assessing the uncertainty of the main nuclear reactions included in the TENDL2012 random data files. A multigroup energy structure of 69 groups is defined, the same as used by the WIMS-D4 code. An example of a random multigroup fission cross-section for ^{235}U and ^{239}Pu is shown in Fig. 3.

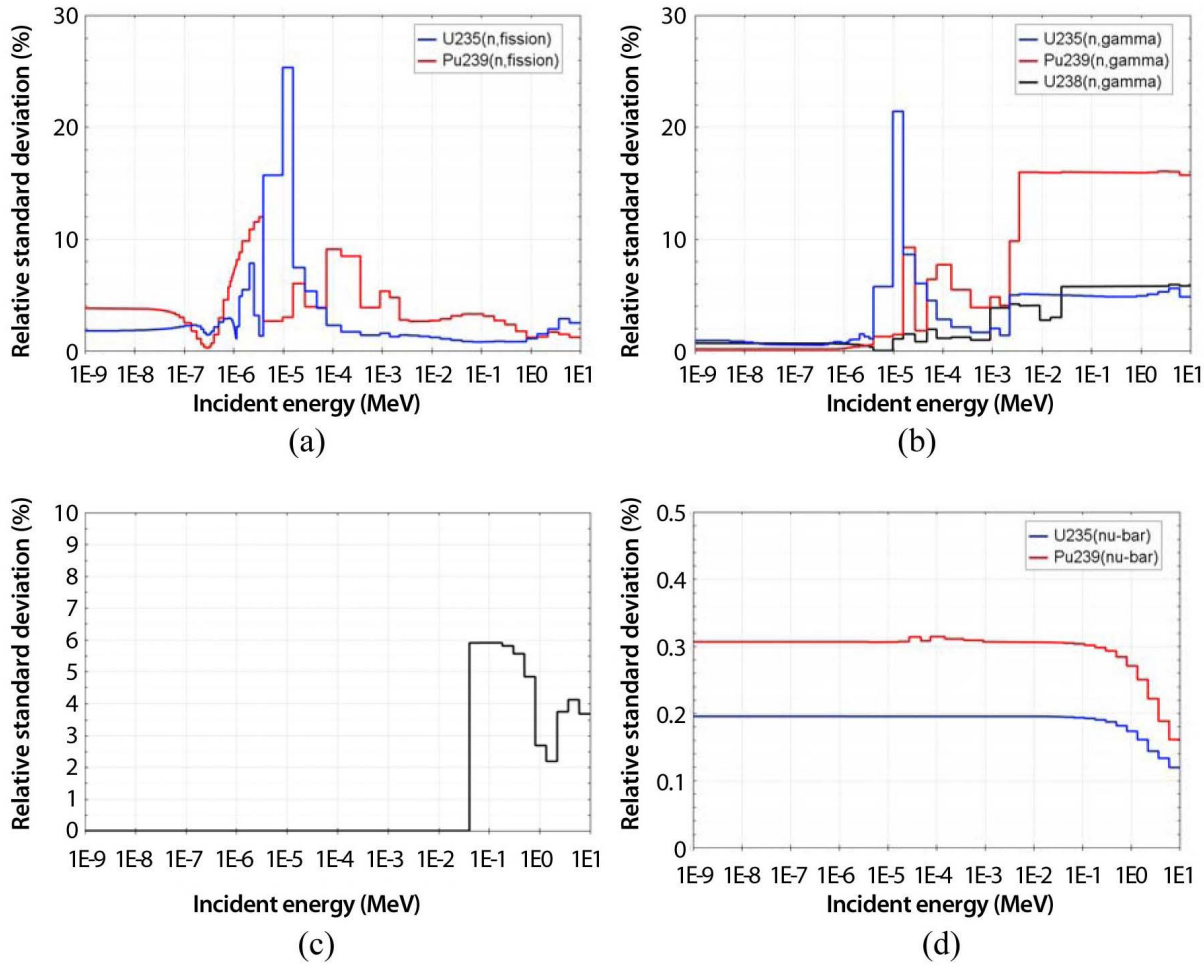

Fig. 4. Multigroup (in 69 Groups) Relative Standard Deviation from Random TENDL2012: (a) (n, Fission) ^{235}U and ^{239}Pu; (b) (n, γ) ^{235}U, ^{238}U and ^{239}Pu; c) Inelastic Scattering of ^{238}U and; (d) (nu-bar) for ^{235}U and ^{239}Pu.

A previous work [15] identified the following reactions as the most important contributors in criticality calculations: ^{239}Pu(nu-bar), ^{238}U(n, γ), ^{238}U(n, n'), ^{239}Pu(n,fission), and ^{235}U(nu-bar) at 30 GWd/MTU. An uncertainty analysis of the ^{235}U, ^{238}U, and ^{239}Pu TENDL2012 random files for these important reactions is presented in Fig. 4.

The large uncertainty around 10 eV for ^{235}U(n, fission) and ^{235}U(n, γ) is remarkable, with relative error values of 25% and 22%, respectively. For ^{239}Pu(n, γ) above 5 keV the uncertainty remains high with a constant value around 16%. The uncertainty for ^{238}U(n, n') is below 6% and the uncertainties for ^{239}Pu(nu-bar) and ^{235}U(nu-bar) reach a nearly constant value below 1 MeV of 0.3% and 0.2%, respectively.

However, discrepancies of these uncertainties are found when comparing with current uncertainty nuclear data libraries, such as SCALE6/UN [7], see Fig. 5. In SCALE6 /UN, uncertainties for ^{235}U(n,fission) and ^{239}Pu(n,fission) remain below 1.4% and 2.6%, respectively. For ^{235}U(n, γ) and ^{239}Pu(n, γ) uncertainties are less than 3% at the thermal neutron energy. For ^{238}U(n, n'), it remains between 5% and 15% below 1 MeV, increasing up to 20-30% above 1 MeV. And, for nu-bar, uncertainty values of 0.3% and 1% for ^{235}U and ^{239}Pu are found.

The random methodology of the incoherent inelastic scattering component of the thermal neutron scattering cross-section for H in H2O was presented in Ref. [11], providing TENDL2012 [10] with a set of random STL files. These files are processed in a multigroup structure with NJOY/GROUPR to obtain the correlation matrix and the relative error. It can be noticed that the uncertainty in the incoherent inelastic scattering cross-section is around 5.8% (see Fig. 6) and a full correlation matrix is found, which is only common for energy-energy correlation matrices obtained from random model parameters [11]. In contrast with this uncertainty value, a negligible uncertainty for the elastic cross-section is found in SCALE6/UN because no uncertainty information in S(α, β) is considered in this library (see Fig. 5e).

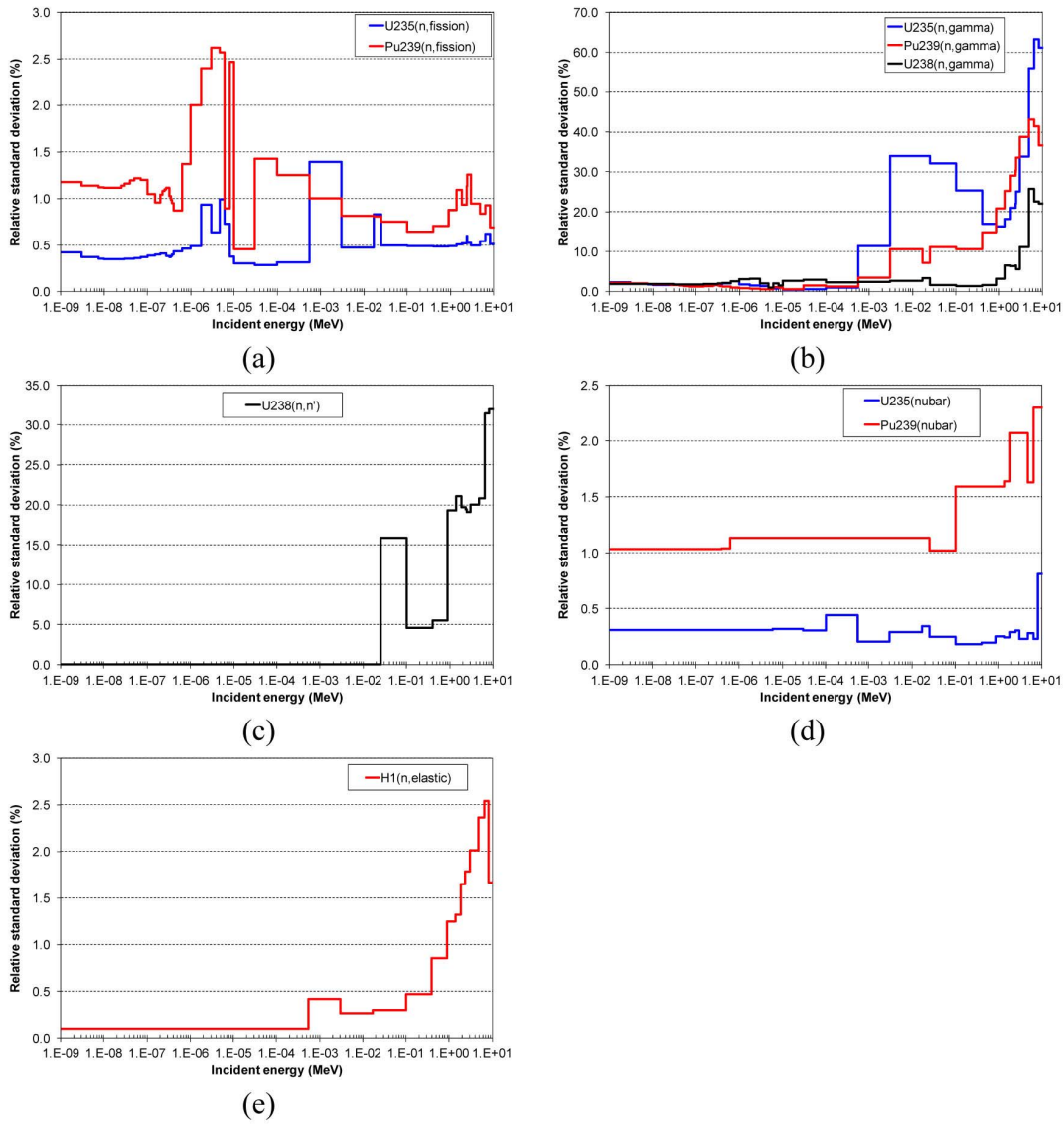

Fig. 5. Multigroup (in 44 Groups) Relative Standard Deviation from SCALE6.1/UN.rev5: (a) (n, Fission) ^{235}U and ^{239}Pu; (b) (n, γ) ^{235}U, ^{238}U and ^{239}Pu; c) Inelastic Scattering of ^{238}U; (d) (nu-bar) for ^{235}U and ^{239}Pu, and e) Elastic Scattering of ^{1}H.

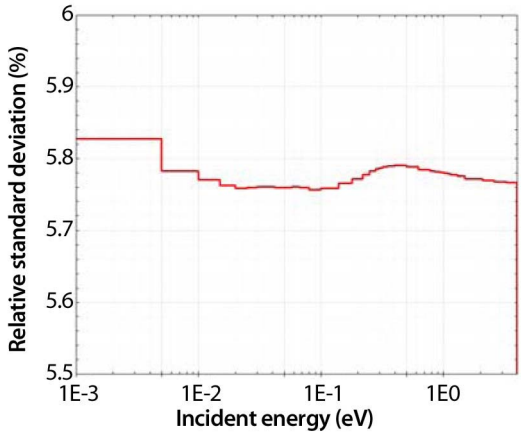

Fig. 6. Uncertainties in the Incoherent Inelastic Scattering Cross Section Calculated from 800 Random TENDL for STL-H in H2O.

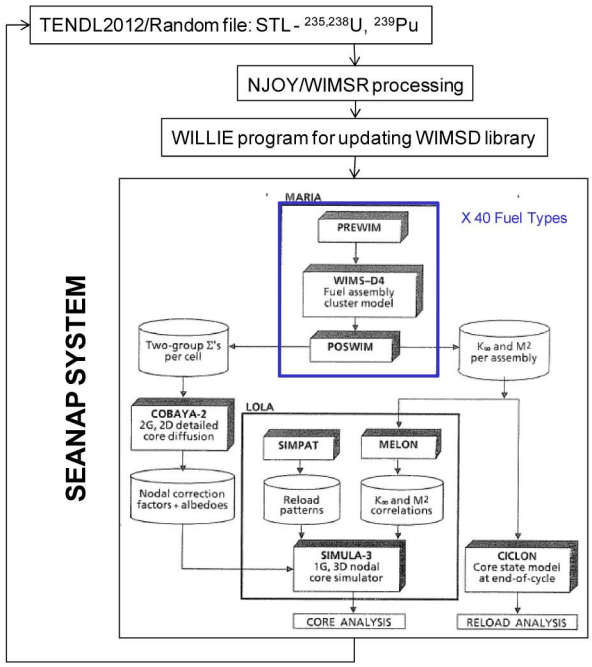

Fig. 7. Scheme of TMC for Random Nuclear Data Analysis

3.2 Methodology

The SEANAP system is repeated for each of the Monte Carlo calculations as shown in Fig. 7. TENDL2012 random files are processed with the NJOY code. The WIMSR module of NJOY is needed to process this file in WIMSD format, and the WILLIE program updates the WIMS-D4 library with the processed random file. Then, the WIMSD random library includes the processed TENDL2012 random file for only one of these materials: H, ^{235}U, ^{238}U or ^{239}Pu. The rest of the materials in the WIMSD random library are the original ones in the reference WIMSD4 library.

After generation of random nuclear libraries, the SEANAP system is used. First, the MARIA sub-system is run for the 40 FA types generating the two-group cross-section and additional data for the COBAYA and SIMULA codes. After *n* SEANAP calculations with *n* different nuclear data libraries, *n* different key parameters of the cycle design with their statistical uncertainties are obtained. The standard deviation reflects the use of different random nuclear data libraries between calculations.

Furthermore, random calculations induce a spread in the distribution of these parameters, which can be assigned to the spread of cross-sections, angular distributions, and so forth in the random nuclear data files. This spread is not known a priori and has to be derived from the present Monte Carlo approach.

An example calculation of Boron Concentration (C_{Boron}) at BOC and HFP with All Rods Out (ARO) is presented in Fig. 8 for 700 random calculations. The first three moments of the distribution (Fig. 8a) are presented as a function of random sampling. It can be seen that the probability distribution is still fluctuating but the impact on the average C_{Boron} and standard deviation (uncertainty) is small. In Fig. 8b, random CBoron is presented as a function of Boron worth (V_{Boron}), Temperature Moderator Coefficient (CTM), Total Peak Power (F_Q), and worth value of the reference bank B inserted (B-IN). This example shows that the TMC method allows easy access to correlations between different design parameters.

4. RESULTS

The first step in the SEANAP system is performed at the fuel assembly level by the MARIA sub-system using the WIMS-D4 code for lattice-cell calculation. The uncertainty information for the different types of FAs in the core is useful to see the impact of uncertainties at this level. In the second step, the whole SEANAP system is used for the analysis of the core design in this cycle including the nominal core depletion, reactivity parameters, reactivity control, and start-up parameters. In both calculations, the impact of nuclear data uncertainties of STL-H in H2O, $^{235\text{-}238}$U, and ^{239}Pu is assessed.

4.1 Uncertainty in Fuel Assembly

A Monte Carlo calculation for a set of 40 different types of FA was performed in this work at BOC-HFP and a boron concentration of 1348 ppm. Table 1 gives the values of average kinf and one standard deviation

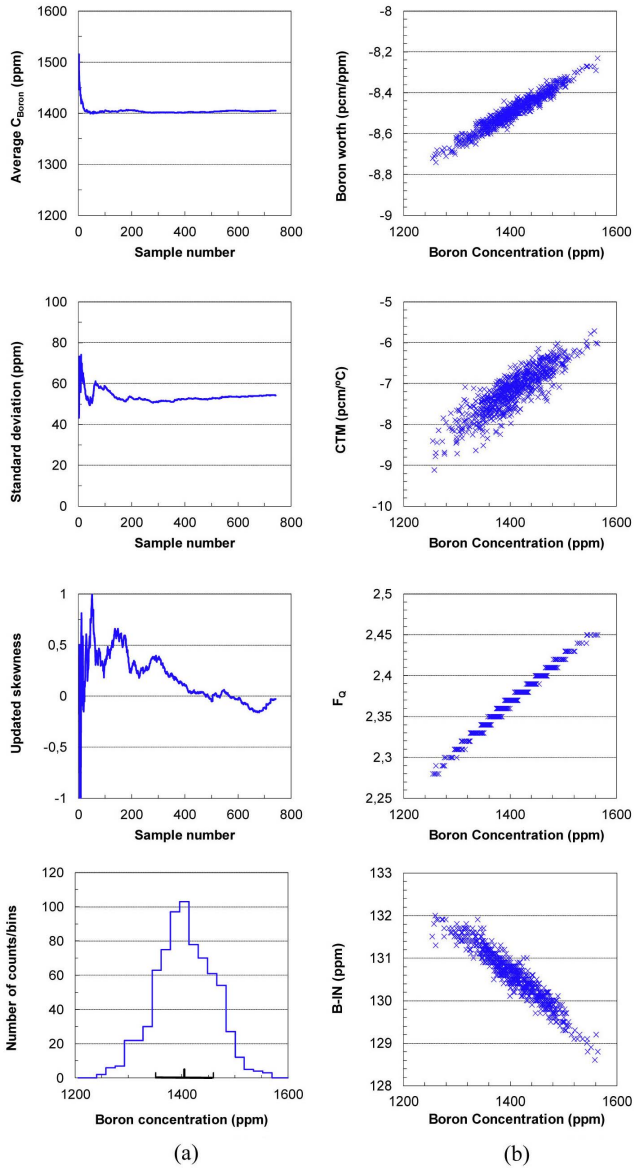

Fig. 8. (a) Example of Convergence for C_{Boron} (ppm) at BOC in the Case of Changing ^{235}U Nuclear Data. Three Moments of the Distribution are Presented: the Average, the Standard Deviation, and the Skewness. b) Example of Correlations between the Inventory of C_{Boron} (ppm) Versus Boron Worth (pcm/ppm), CTM (pcm/ºC), F_Q and B-IN (ppm) at BOC, Obtained by Randomizing the ^{235}U Transport Nuclear Data.

(uncertainty) varying the neutron transport data for STL-H in H2O, ^{235,238}U, and ^{239}Pu, where the total contribution to all of them is shown in the last column.

The uncertainty propagation in FA reactivity can be summarized as follows:

- For STL-H in H2O, since it affects the thermalization of neutrons, a large impact in the uncertainty is found where control rods are inside the FA, being the most important contributor to the total uncertainty for these cases. A large effect is found for B4C control rods for FA#32 and FA#36, reaching an uncertainty of 0.69 Δk/k%. Both burnable absorbers and burnup induce an increase of uncertainty.
- For ^{239}Pu, the uncertainty contribution becomes more important at higher burnups, being the most important contributor above 20 GWd/tHM. The effect also increases with low enrichment. FA#2 has the maximum contribution with 0.52 Δk/k%.
- In the case of ^{235}U and ^{238}U, they have a large impact along cycle operation. For ^{238}U, a nearly constant contribution of 0.27 Δk/k% is found in all the FAs. This makes the uncertainty of ^{235}U one of the most important contributors, especially for low burnups. The maximum contribution of ^{235}U is for FA#22 with 0.66 Δk/k%.
- The sum of contributions for FA without control rods is between 0.60-0.73 Δk/k%. With control rods the total uncertainty is in the range 0.80-0.93 Δk/k%.

4.2 Uncertainty in Core Parameters for Nuclear Design

The results of randomizing SEANAP for a nominal cycle operation are presented in Fig. 9 for the following core parameters: boron concentration, axial power distribution, and peak power factors; reactivity coefficients are presented in Fig. 10 and integral reactivity of control banks at the startup in Table 2. This comparison is useful to assess the impact of nuclear data uncertainties in core analysis design.

- Total boron concentration uncertainty decreases from 70 ppm at BOC to 55 ppm at EOC. ^{235}U and ^{239}Pu are the most important contributors. For ^{239}Pu, as the thermal fission rate increases for high burnups, its uncertainty increases as a function of burnup. On the contrary, the uncertainty of ^{235}U decreases from 59 ppm to 29 ppm. Both ^{238}U and STL-H in H2O slowly decrease as a function of burnup.

This large uncertainty can be attributed to the large uncertainty at the thermal energy for the fission cross-sections with ^{235}U and ^{239}Pu.

- AO uncertainty is only important at BOC, with a total deviation less than 2%. STL-H in H2O and ^{238}U are the most important contributors.
- Uncertainties for maximum peak power distributions F_z, $F_{\Delta H}$, and F_Q always remain less than 2% at BOC, showing a negligible effect for high burnup.
- Boron worth uncertainty has a deviation of nearly ~0.90 pcm/ppm with a negligible effect due to STL-H in H2O.
- Isothermal and temperature moderator reactivity coefficients increase their uncertainty as a function of burnup. At BOC-HZP, where these values are critical, uncertainties are: 2.21 pcm/ºC for CTM, 2.65 pcm/ºC for CISO, and 1.71 pcm/ºC for CDOP, with ^{238}U as the most important contributor. Uncertainty

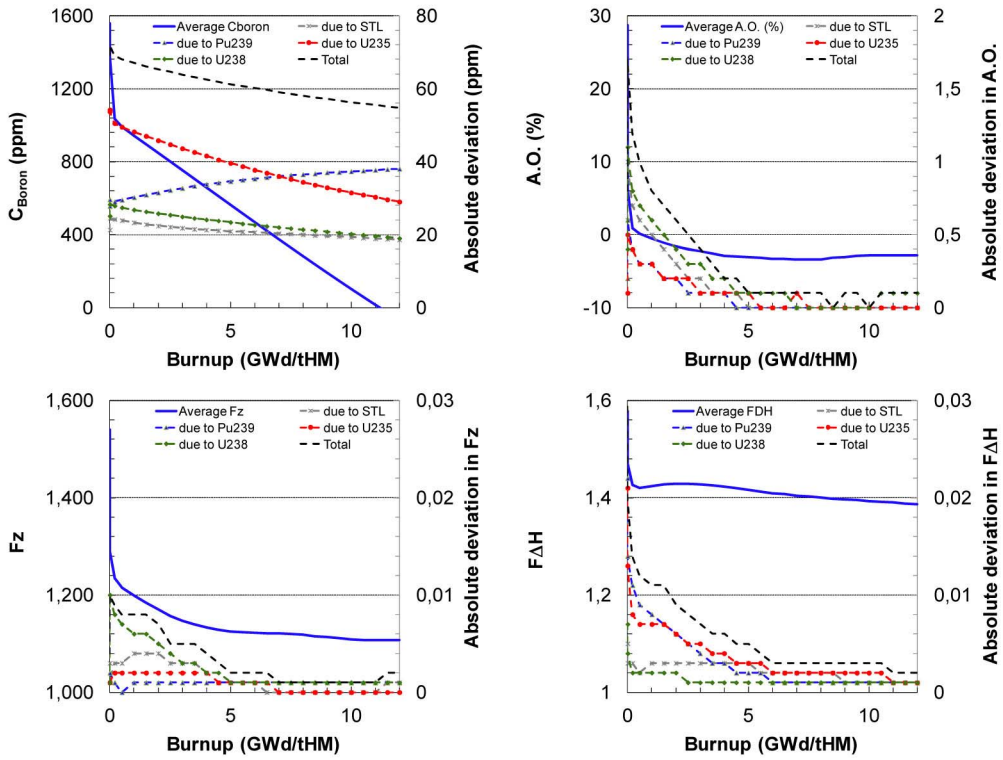

Fig. 9. Average Value and Absolute Deviation (Uncertainty) as a Function of the Burnup for C_{Boron}, Axial Offset (A.O.), F_z and $F_{\Delta H}$. Uncertainty for Each of the Nuclear Data Varied (STL-H in H2O, ^{235,238}U and ^{239}Pu) and the Sum of the Different Contributions.

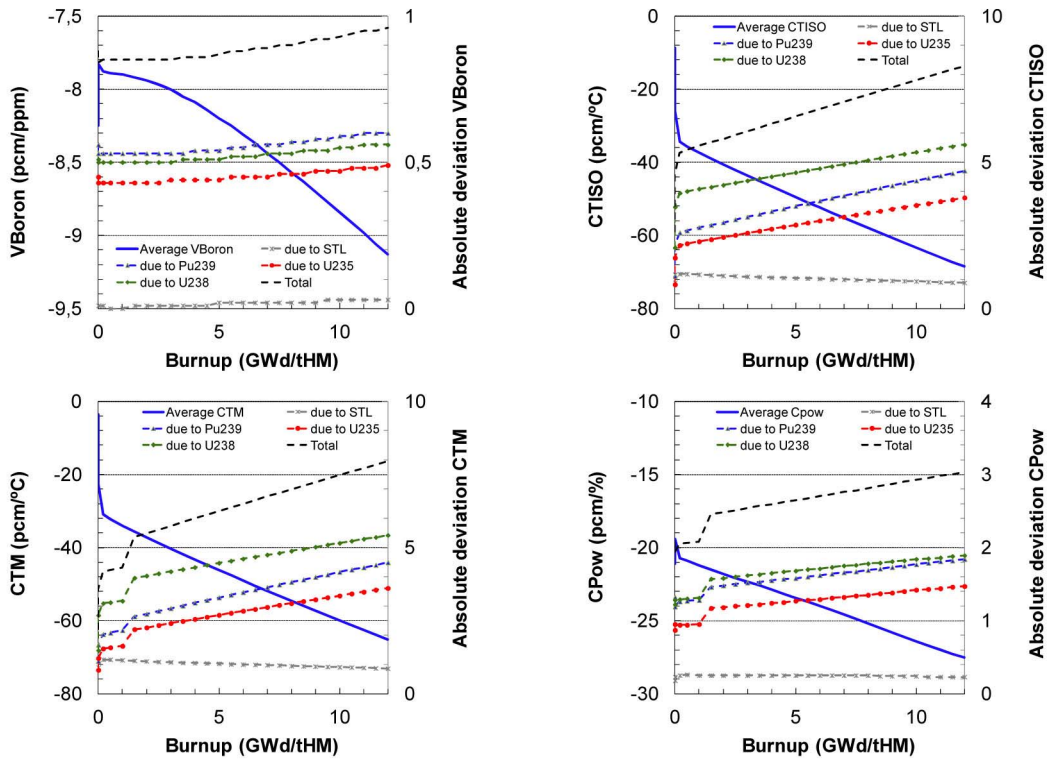

Fig. 10. Average Value and Absolute Deviation (Uncertainty) as a Function of the Burnup for Boron Worth, Isothermal, Temperature Moderator and Power Reactivity Coefficients. Uncertainty for Each of the Nuclear Data Varied (STL-H in H2O, ^{235,238}U and ^{239}Pu) and the Sum of the Different Contributions.

for power reactivity is in the range of 2-3 pcm/%.

- In Table 2, control bank worths are reported at BOC-HZP. Uncertainty for the reference bank B is only 2 ppm, equivalent to an uncertainty of 16.5 pcm.

4.3 Uncertainty Calculations in Comparison with Measurements

However, validation by an extensive comparison with measurements at cycle start-up tests (end-point boron concentrations, isothermal temperature coefficients, differential and integral worth of control rod banks) and along cycle nominal operation (critical boron concentrations and 1D or 2D power distributions) is needed for the qualification of any computer system for 3D PWR core analysis. Thus, the SEANAP system has been extensively validated with an experimental database accumulated from about 70 cycles of 6 PWR units operating in Spain.

To assure the adequacy of these calculations, the deviations between measured and calculated values are used. In Table 3, a summary of the Westinghouse- PWR design and acceptance criteria for the most relevant core parameters are illustrated. This comparison can be useful to check the fuel loading pattern and control rod configuration.

In this work, a comparison of these design and acceptance criteria with the uncertainties of calculated values is performed. This comparison is useful to assess the impact of nuclear data uncertainties on these safety criteria. In Tables 4 and 5, an analysis for C_{Boron} and AO is shown, providing two different types of calculated value.

Table 2. Average Value and Absolute Deviation (Uncertainty) as a Function of the Burnup for Control Bank Worth. Uncertainty for Each of the Nuclear Data varied (STL-H in H2O, ^{235,238}U and ^{239}Pu) and the Sum of the Different Contributions

	Average (ppm)	Absolute standard deviation (ppm)				
		STL	^{239}PU	^{235}U	^{238}U	Total
D-IN	**120.3**	1.3	0.5	0.7	0.7	1.7
C-IN	**92.2**	0.8	2.6	1.4	1.1	3.2
B-IN	**138.1**	0.9	0.5	1.6	0.8	2.0
A-IN	**92.3**	0.5	3.5	3.9	0.7	5.3
SB-IN	**88.9**	1.1	3.3	2.4	1.4	4.5
SA-IN	**120.3**	0.8	2.3	3.2	0.6	4.0
D+C-IN	**237.8**	2.1	2.9	0.7	1.6	4.0
D+C+B-IN	**419.2**	3.5	4.5	1.0	2.4	6.2
D+C+B+A-IN	**565.2**	4.1	1.6	6.5	1.7	8.0
D+C+B+A+SB-IN	**701.8**	5.6	2.8	3.9	2.9	7.9
ARI	**917.5**	7.8	2.6	5.4	3.2	10.3

Table 3. Design and Acceptance Criteria for Start-up and Operation

Core parameter	**Design criteria**	**Acceptance criteria**
Critical boron concentration ARO	$\lvert(C_B)^M_{ARO}-(C_B)^C_{ARO}\rvert$ <50 ppm	$\lvert\alpha C_B \times \Delta(C_B)_{ARO}\rvert$< 1000 pcm
Isothermal temperature coefficient ARO at HZP	$\lvert(\alpha^{ISO_T})^M_{ARO}-(\alpha^{ISO_T})^C_{ARO}\rvert$ <3.6 pcm/ºC	$\lvert(\alpha^{ISO_T})^M_{ARO}-(\alpha^{ISO_T})^C_{ARO}\rvert$ <6.62 pcm/ºC
Moderator temperature coefficient ARO at HZP	$(\alpha^{CTM})^{HZP}_{ARO}$ <9 pcm/ºC	
Boron Worth Coefficient at HZP	$\lvert(\alpha C_B)^M-(\alpha C_B)^C\rvert$< 0.7 pcm/ppm	
Control banks worth for Reference Bank	$\lvert(I^{REF})^M-(I^{REF})^C\rvert$ <0.10x$(I^{REF})^C$	$\lvert(I^{REF})^M-(I^{REF})^C\rvert$ <0.15x$(I^{REF})^C$
Control Bank Worth value for other Banks using Rod Swap Technique	$\lvert(I^{CBW})^M-(I^{CBW})^C\rvert$ <0.15x$(I^{CBW})^C$ or 100 pcm	$\lvert(I^{CBW})^M-(I^{CBW})^C\rvert$ <0.30x$(I^{CBW})^C$ or 200 pcm
Total Control Bank Worth	1.10 x$(I^{TOT})^C$ > $(I^{TOT})^M$ >0.9x$(I^{TOT})^C$	$(I^{TOT})^M$ >0.9x $(I^{TOT})^C$
Axial Offset	$\lvert(AO)^M-(AO)^C\rvert$< 3%	
Max. Relative Assembly Power (P_A)	% $\lvert(P_A)^M-(P_A)^C\rvert/(P_A)^C$ { < 10% if P ≥90%; < 15% if P<90%	

Table 4. Measured Boron Concentrations (ppm) and Calculated Values Versus Cycle Operation. Calculated Values with Different Nuclear Data libraries: WIMS-D4 Reference Library, and Updated WIMS-D4 Library with Random TENDL2012 Files of STL-H in H2O or ^{239}Pu. Average and Absolute Deviation in ppm for Random Calculations.

Power (%)	Burnup (GWd/tHM)	Meas.	WIMS-D4		STL			Pu239		
			C	M-C	C_Avg	Abs. Dev.	M-C	C_Avg	Abs. Dev	M-C
50	0.015	1200	1141	59	1184	22	16	1149	28	51
75	0.031	1113	1062	51	1107	23	7	1070	29	43
100	0.134	985	990	-5	1035	24	-50	998	29	-13
100	1.34	870	883	-13	927	24	-57	892	31	-22
100	2.487	779	787	-8	830	23	-51	797	33	-18
100	2.842	755	758	-3	801	23	-46	768	34	-13
100	3.591	688	691	-3	732	23	-44	701	35	-13
100	4.441	604	617	-13	657	23	-53	627	36	-23
100	5.549	504	514	-10	552	23	-48	524	38	-20
100	6.692	412	405	7	443	23	-31	416	40	-4
100	7.716	319	305	14	341	23	-22	315	41	4
100	8.823	227	201	26	235	23	-8	211	42	16
100	10.284	101	57	44	90	23	11	68	44	33
100	11.351	4	-51	55	-19	23	23	-41	45	45

Table 5. Measured Axial Offset (%) and Calculated Values Versus Cycle Operation. Calculated Values with Different Nuclear Data Libraries: WIMS-D4 Reference Library, and Updated WIMS-D4 Library with Random TENDL2012 Files of STL-H in H2O or ^{239}Pu. Average and Absolute Deviation in ppm for Random Calculations.

Power (%)	Burnup (GWd/tHM)	Meas.	WIMS-D4		STL			Pu239		
			C	M-C	C_Avg	Abs. Dev.	M-C	C_Avg	Abs. Dev	M-C
50	0.015	7.7	4.8	2.9	5.7	0.5	2.0	4.9	0.2	2.8
75	0.031	3.8	2.7	1.1	3.8	0.6	0.0	2.9	0.3	0.9
100	0.134	-0.7	-0.7	0.0	0.7	0.7	-1.4	-0.5	0.4	-0.2
100	1.34	-1.6	-2.0	0.4	-1.2	0.4	-0.4	-1.9	0.2	0.3
100	2.487	-2.4	-3.0	0.6	-2.6	0.2	0.2	-3.0	0.1	0.6
100	2.842	-2.8	-3.0	0.2	-2.7	0.2	-0.1	-3.0	0.1	0.2
100	3.591	-3.8	-4.3	0.5	-4.1	0.1	0.3	-4.2	0.1	0.4
100	4.441	-3.2	-3.2	0.0	-3.1	0.1	-0.1	-3.2	0.0	0.0
100	5.549	-3.9	-3.7	-0.2	-3.7	0.0	-0.2	-3.7	0.0	-0.2
100	6.692	-4.2	-3.8	-0.4	-3.8	0.0	-0.4	-3.8	0.0	-0.4
100	7.716	-4.7	-4.3	-0.4	-4.4	0.0	-0.3	-4.3	0.0	-0.4
100	8.823	-3.6	-2.4	-1.2	-2.4	0.0	-1.2	-2.4	0.0	-1.2
100	10.284	-3.5	-1.6	-1.9	-1.6	0.0	-1.9	-1.6	0.0	-1.9
100	11.351	-3.4	-2.0	-1.4	-2.1	0.0	-1.3	-2.0	0.0	-1.4

Firstly, a standard SEANAP system calculation is performed with the reference WIMSD library. In this case, the design criteria are achieved except for the case of boron concentration at 50% of power-BOC. However, the acceptance criteria are met. Secondly, two additional calculations are performed, each case modifying only the library for ^{239}Pu or STL-H in H2O. These updates use the random set of files provided by TENDL2012. Then, the average value and absolute deviation (uncertainty) can be predicted. In both cases, the design criteria are achieved except for boron concentration at BOC when STL-H in H2O is varied.

Regarding the absolute deviation of these calculations, a high uncertainty can be seen in the prediction of boron concentration. For the case of ^{239}Pu, from 28 ppm at BOC and increasing until 45 ppm at EOC, and for STL-H in H2O, a nearly constant uncertainty of ~22 ppm is found. The uncertainty of A.O. remains below 1% in both cases.

Another important analysis is the comparison between the baseline calculation (C) from WIMS-D4 and the mean value from samples (C_Avg). In Table 4, the baseline calculation (C) of boron concentration is consistently lower that the mean value from STL samples (C_Avg), where values range from ~10-50 ppm. It shows a difference between the TENDL2012 and WIMS-D4 scattering cross-section of H in H2O, where a higher scattering cross-section in TENDL2012 induces a softer neutron spectra increasing the core reactivity. For ^{239}Pu, the mean values from ^{239}Pu samples are ~10 ppm above the baseline calculation (C). The difference between TENDL2012 and WIMS-D4 nuclear data in ^{239}Pu generates these differences. In Table 5, the baseline calculation (C) of A.O. agrees with the ^{239}Pu mean values. For STL samples, the mean values begin ~1% larger than the baseline calculation (C), then they gradually converge to baseline with higher burnup.

The influence of nuclear data uncertainties on core power distributions has been investigated. Table 6 gives the differences in the assembly relative powers distribution calculated by SIMULA with the measured values at BOC-HFP-ARO and Xenon equilibrium. The assembly power acceptance criterion is met, with differences below 6%.

Table 6. Relative Percentage Assembly Power ((M-P)/P·100) Core Distribution between Measured (M) and Predicted (P) Values at BOC-HFP and Xenon Equilibrium using WIMS-D4 library and Random TENDL Files (STL-H for H2O and ^{239}Pu). Relative Error in % for Random Cases is Provided.

5.3	3.7	4.9	-0.6	1.9	-1.8	-0.3	1.9	WIMS-D4
5.9±0.1	4.1±0.2	5.6±0.2	0.0±0.2	2.2±0.0	-1.8±0.0	-0.9±0.1	1.6±0.0	Random STL
4.8±1.8	3.3±1.4	4.5±1.3	-0.7±0.4	1.8±0.4	-1.6±0.6	-0.2±0.6	2.1±0.7	Random ^{239}Pu
3.4	2.2	2.8	4.6	1.0	0.5	-1.3	3.4	
3.8±0.2	2.6±0.1	3.3±0.2	5.2±0.2	1.1±0.1	0.4±0.0	-1.6±0.1	3.1±0.0	
3.0±1.4	1.7±1.4	2.5±1.1	4.3±0.8	1.0±0.2	0.6±0.2	-0.9±1.1	3.4±0.6	
4.0	2.2	4.6	-1.6	0.0	-1.6	-0.4		
4.7±0.2	2.6±0.2	5.2±0.1	-1.2±0.1	-0.1±0.1	-1.9±0.1	-0.7±0.1		
3.6±1.3	1.8±1.1	4.4±1.0	-1.6±0.2	-0.1±0.2	-1.3±0.8	0.0±1.3		
-1.7	3.5	-1.9	0.0	-1.4	-2.0	2.5		
-1.1±0.2	4.1±0.2	-1.6±0.1	0.0±0.1	-1.9±0.2	-2.3±0.2	2.0±0.0		
-1.8±0.4	3.2±0.8	-1.9±0.2	-0.2±0.5	-1.5±0.1	-1.7±0.8	2.5±0.7		
0.4	-0.4	-1.0	-2.3	-1.8	-0.7			
0.8±0.0	-0.3±0.1	-1.0±0.1	-2.7±0.2	-2.4±0.3	-1.2±0.2			
0.3±0.4	-0.5±0.2	-1.1±0.2	-2.4±0.1	-1.9±0.1	-0.7±0.2			
-3.1	-1.0	-2.9	-2.6	-1.0				
-3.1±0.0	-1.2±0.0	-3.2±0.1	-2.9±0.2	-1.5±0.3				
-2.9±0.6	-1.0±0.2	-2.6±0.8	-2.3±0.8	-1.0±0.2				
-0.8	-2.0	-1.5	0.5					
-1.4±0.1	-2.2±0.1	-1.6±0.1	0.2±0.0					
-0.7±0.6	-1.6±1.1	-1.0±1.3	0.7±0.7					
1.6	3.1							
1.2±0.0	3.1±0.0							
1.9±0.7	3.4±0.6							

The uncertainty calculation is dominated by ^{239}Pu, with a maximum value of 1.8% at the centre of the core.

Comparison between the baseline calculation (C) from WIMS-D4 and the mean value from samples (C_Avg) shows a tilt effect across this core map. For STL samples (C_Avg), a positive bias of +0.6% can be found at the center of the core to about -0.5% at the edges. This effect is related to the differences between TENLD2012 and WIMS-D4 for H in H2O scattering cross-section. Using TENDL2012 STL samples, the center of the reactor core exhibits high neutron thermalization, and the power distribution at the center is increased. However, the ^{239}Pu mean value from samples (C_Avg) tilts in the opposite direction with a negative bias near the center of -0.5% and a positive bias near the edges of +0.3%. The difference between TENDL2012 and WIMS-D4 nuclear data in ^{239}Pu is the reason for this tilt.

5. CONCLUSION

Nowadays, the methodology to predict the calculational uncertainty in a core analysis system is based on an extensive validation of the calculated results and the measured and design data at cycle start-up tests and nominal operation. However, this calculational uncertainty ignores the term due to the uncertainty in the nuclear data. In this paper we have analyzed the uncertainty of some safety core design parameters for a typical PWR in terms of the uncertainties due to nuclear data in ^{235,238}U, ^{239}Pu, and STL-H in H_2O. To perform this uncertainty propagation study, a Monte Carlo method was applied, repeating similar calculations using a set of random nuclear data files, TENDL2012/random.

Since the global uncertainties are within the design and acceptable criteria, it can be concluded that calculation uncertainties due to nuclear data ensure bounding estimates in safety margins. However, uncertainties of 50-60 ppm in the boron concentration, close to the design criteria, suggest that nuclear data uncertainties in TENDL2012 are still large compared with other uncertainty data.

An analysis of significant differences between the uncertainty data of TENDL2012/random and SCALE6 /UN has identified several questions to be explained by using the TMC methodology: i) large uncertainty in the range 1eV-100eV for fission and captures reactions in ^{235,238}U and ^{239}Pu, ii) low uncertainties in the (n,n') reaction of ^{238}U compared with the estimations in evaluated files, and decreasing its uncertainty at higher neutron energies, and iii) larger uncertainty for ^{239}Pu(nu-bar), and again these nu-bar uncertainties decrease at higher neutron energies.

Thus, a depth uncertainty analysis for these important reactions is required in random TENDL libraries. Year after year the quality of the TENDL library has been improved through adjustments of TALYS input parameters. But, validation of random files will require much effort.

ACKNOWLEDGMENTS

This work was performed in the framework of the agreement in the area of Propagation of Uncertainties for Neutronic Calculations (P110530207) in Criticality Safety Analysis between the Spanish Nuclear Safety Council (CSN) and the Universidad Politécnica de Madrid (UPM). The authors wish to thank Dr. D. Rochman from NRG (The Netherlands) for the motivation and support, providing random TENDL files needed for this work.

REFERENCES

[1] C. Ahnert, J.M. Aragonés, "Fuel Management and Core Design Code Systems for PWR Neutronic Calculations", *Nucl. Technol*., **69**, 350 (1985)

[2] J. M. Aragonés, C. Ahnert, "A Linear Discontinuos Finite Difference Formulation for Synthetic Coarse-Mesh Few-Group Diffusion Calculations", *Nucl. Sci. Eng*., **94**, 309 (1986)

[3] C. Ahnert, J.M. Aragonés, O. Cabellos, N. García-Herránz, "Continuous Validation and Development for Extended Applications of the SEANAP Integrated 3-D PWR Core Analysis System", in Mathematics and Computation, Reactor Physics and Environmental Analysis in Nuclear Applications, J.M. Aragonés (Ed.), Vol. **1**, 710-719, Senda Ed., Madrid (1999).

[4] W. Zwermann, B. Krzykacz-Hausmann, L. Gallner, A. Pautz and M. Mattes, "Uncertainty Analyses with Nuclear Covariance Data in Reactor Core Calculations", *J. of the Korean Physical Soc*., **59**, No. 2, pp. 1256-1259, (2011)

[5] O. Buss, A. Hoefer, J.C. Neuber , "Nuduna: Towards a Complete Nuclear Data Uncertainty Estimation for Criticality Safety Applications", International Conference on Nuclear Criticality 2011, Edinburgh (2011)

[6] A.J. Koning, D. Rochman, "Towards Sustainable Nuclear Energy: Putting Nuclear Physics to work", *Ann. Nuclear Energy*, **35**, 2024 (2008)

[7] B. T. Rearden, M. L. Williams, M. A. Jessee, D. E. Mueller, D. A. Wiarda, "Sensitivity and Uncertainty Analysis Capabilities and Data in SCALE", *Nuclear Technology*, **174**, No. 2, pp. 236-288 (2011)

[8] Ho Jin Park, Hyung Jin Shim and Chang Hyo Kim, "Uncertainty Propagation in Monte Carlo Depletion Analysis," *Nucl. Sci. Eng*., **167**, 196-208 (2011)

[9] D. Rochman, A.J. Koning, D.F. Da CRUZ, "Propagation of ^{235,236,238}U and ^{239}Pu Nuclear Data Uncertainties for a Typical PWR Fuel Element", *Nuclear Technology*, **179**, 323-338, (2012)

[10] A. J. Koning and D. Rochman, "Modern Nuclear Data Evaluation With The TALYS Code System", *Nuclear Data Sheets*, **113**, 2841-2934 (2012)

[11] D. Rochman and A. J. Koning, "Random Adjustment of the H in H2O Neutron Thermal Scattering Data", *Nuclear Science and Engineering*, **172**, 287–299 (2012)

[12] M.J. Halsall, " A Summary of WIMS-D4 Input", AEEW-M-1327, U.K. Atomic Energy Establishment, Winfrith (1980)

[13] R.E. McFarlane, "*NJOY99- Code System for Processing Pointwise and Multigroup Neutron and Photon Cross Sections from ENDF/B Data*", RSIC PSR-480, Los Alamos National Laboratory, (2000)

[14] A. Trkov, "WILLIE Program, Operations on WIMS cross section library", IAEA-1408: WLUP3.0, 69 and 172 Group

Cross Section Libraries for WIMS, (2008)
[15] O. Cabellos, "Presentation and Discussion of the UAM/ Exercise I-1b: "Pin-Cell Burn-Up Benchmark" with the Hybrid Method," *Science and Technology of Nuclear Installations*, vol. **2013**, Article ID 790206, 12 pages, 2013. doi:10.1155/2013/790206